



The Second International Asteroid Warning Network Timing Campaign: 2005 LW3

Davide Farnocchia¹, Vishnu Reddy², James M. Bauer³, Elizabeth M. Warner³, Marco Micheli⁴, Matthew J. Payne⁵,
 Tony Farnham³, Michael S. Kelley⁶, Miguel R. Alarcon^{7,8}, Paolo Bacci⁹, Roberto Bacci^{9,10}, Mauro Bachini^{11,12},
 Kevin Baillie¹³, Giorgio Baj¹⁴, Daniel Bamberger¹⁵, Anatoly P. Barkov¹⁶, Stefan Beck¹⁷, Guido Betti¹⁸,
 Enrico Biancalani^{19,20,21}, Bryce T. Bolin^{22,23,24}, David Briggs²⁵, Luca Buzzi²⁶, Haowen Cheng²⁷, Eric Christensen²,
 Alessandro Coffano²⁸, Luca Conversi⁴, Christophe Demeautis²⁹, Larry Denneau³⁰, Josselin Desmars^{13,31},
 Anlaug A. Djupvik^{19,20}, Leonid Elenin³², Paolo Fini¹⁸, Tobias Felber³³, Randy Flynn³⁴, Gianni Galli³⁵,
 Mikael Granvik^{36,37}, Bill Gray³⁸, Zuri Gray^{19,39,40}, Luca Grazzini⁴¹, Werner Hasubick⁴², Tobias Hoffmann⁴³,
 Robert Holmes⁴⁴, Marco Iozzi⁴⁵, Alexander L. Ivanov¹⁶, Viktor A. Ivanov¹⁶, Natalya V. Ivanova¹⁶, Cristóvão Jacques⁴⁶,
 Hai Jiang²⁷, Zheng Jinghui⁴⁷, Anni Kasikov^{19,20,48}, Myung-Jin Kim⁴⁹, Balaji Kumar⁵⁰, Hee-Jae Lee⁴⁹, Bin Li^{51,52},
 Jing Liu²⁷, Javier Licandro^{7,8}, Tyler Linder⁴⁴, Vadim E. Lysenkov¹⁶, Martina Maestripietri⁹, Andrea Mantero⁵³,
 Vladimiro Marinello²⁸, Jennie McCormick⁵⁴, Darrel Moon⁵⁵, Alessandro Nastasi⁵⁶, James D. Neill²², Guenther Neue⁵⁷,
 Artem O. Novichonok⁵⁸, Francisco Ocaña⁴, Gianpaolo Pizzetti²⁸, Anton Pomazan⁴⁷, Josiah N. Purdum²², Christophe Ratinand⁵⁹,
 Dong-Goo Roh⁴⁹, Philipp D. Romanov^{60,61,62,63}, Nello Ruocco⁶⁴, Toni Santana-Ros^{65,66}, Toni Scarmato⁶⁷,
 Anastasia Schmalz³², Sergei Schmalz³², Miquel Serra-Ricart^{7,8}, Clay Sherrod⁶⁸, Nick Sioulas⁶⁹, Andrea Soffiantini²⁸,
 Giacomo Succi^{11,12}, David J. Tholen³⁰, Jeppe S. Thomsen^{19,20,70}, William Thuillot¹³, Richard Wainscoat³⁰, Guy Wells¹⁵,
 Robert Weryk⁷¹, Nikolai A. Yakovenko¹⁶, Hong-Suh Yim⁴⁹, and Chengxing Zhai¹

¹ Jet Propulsion Laboratory, California Institute of Technology, 4800 Oak Grove Dr., Pasadena, CA 91109, USA; Davide.Farnocchia@jpl.nasa.gov

² Lunar and Planetary Laboratory, University of Arizona, 1629 E. University Blvd., Tucson, AZ 85721, USA

³ University of Maryland, 4296 Stadium Dr., Astronomy Dept. Room 1113, College Park, MD 20742, USA

⁴ ESA NEO Coordination Centre, Largo Galileo Galilei, 1, I-00044 Frascati (RM), Italy

⁵ Harvard-Smithsonian Center for Astrophysics, 60 Garden St., MS 51, Cambridge, MA 02138, USA

⁶ Planetary Defense Coordination Office, Planetary Science Division, NASA Headquarters, 300 E St. SW, Washington, DC 20546, USA

⁷ Instituto de Astrofísica de Canarias, C/ Vía Láctea s/n, E-38205 La Laguna, Canarias, Spain

⁸ Departamento de Astrofísica, Universidad de La Laguna, E-38206 La Laguna, Canarias, Spain

⁹ GAMP—Osservatorio Astronomico Montagna Pistoiense, Via Pratorsi, I-51028 San Marcello Piteglio (PT), Italy

¹⁰ G. Pascoli Observatory, Via dei Pieri, I-55051 Castelvecchio Pascoli (LU), Italy

¹¹ Tavolaia Observatory, Via Tavolaia 4, I-56020 Santa Maria A Monte (PI), Italy

¹² BS-CR Observatory, Via Francesca 329, I-56020 Santa Maria A Monte (PI), Italy

¹³ IMCCE, Paris Observatory, PSL University, CNRS, Sorbonne University, Lille University, 77 av. Denfert-Rochereau, F-75014 Paris, France

¹⁴ Observatory M57, Via Viggù 35, I-21050 Saltrio (VA), Italy

¹⁵ Northolt Branch Observatories, Dabbs Hill Lane, Northolt, London, UK

¹⁶ Kuban State University, Stavropolskaya St., 149, Krasnodar 350040, Russia

¹⁷ Altdorf Observatory, Eschelbachstr. 17, D-71088 Holzgerlingen, Germany

¹⁸ Observatory Beato Ermanno, Via Sodera 2, I-50023 Impruneta (FI), Italy

¹⁹ Nordic Optical Telescope, Rambla José Ana Fernández Pérez 7, E-38711 Breña Baja, Spain

²⁰ Department of Physics and Astronomy, Aarhus University, Ny Munkegade 120, DK-8000 Aarhus C, Denmark

²¹ Leiden Observatory, Leiden University, P.O. Box 9513, NL-2300 RA Leiden, The Netherlands

²² Division of Physics, Mathematics, and Astronomy, California Institute of Technology, 1200 E. California Blvd., Pasadena, CA 91125, USA

²³ Infrared Processing and Analysis Center, California Institute of Technology, 1200 E. California Blvd., Pasadena, CA 91125, USA

²⁴ Goddard Space Flight Center, 8800 Greenbelt Rd., Greenbelt, MD 20771, USA

²⁵ Hampshire Astronomical Group, Clanfield, Hampshire, UK

²⁶ Schiaparelli Astronomical Observatory, Via Orrigoni 4, I-21100 Varese (VA), Italy

²⁷ National Astronomical Observatories, Chinese Academy of Sciences, 20A Datun Rd., Chaoyang District, Beijing, People's Republic of China

²⁸ Serafino Zani Observatory, Consortile San Nicola, I-25065 Lumezzane (BS), Italy

²⁹ PASTIS Observatory, F-04150 Banon, France

³⁰ Institute for Astronomy, University of Hawaii, 2680 Woodlawn Dr., Honolulu, HI 96822, USA

³¹ Institut Polytechnique des Sciences Avancées IPSA, 63 boulevard de Brandebourg, F-94200 Ivry-sur-Seine, France

³² Keldysh Institute of Applied Mathematics, Russian Academy of Sciences, Miusskaya sq. 4, Moscow, 125047, Russia

³³ Oberfrauendorf Observatory, An der Lockwitz 52, D-01768 Glashütte, Germany

³⁴ Squirrel Valley Observatory, 3870 River Rd., Columbus, NC 28722, USA

³⁵ GiaGa Observatory, Via Mozart 4, I-20005 Pogliano Milanese (MI), Italy

³⁶ Department of Physics, P.O. Box 64, FI-00014 University of Helsinki, Finland

³⁷ Asteroid Engineering Lab, Luleå University of Technology, Box 848, SE-98128 Kiruna, Sweden

³⁸ Project Pluto, 168 Ridge Rd., Bowdoinham, ME 04008, USA

³⁹ Armagh Observatory and Planetarium, College Hill, Armagh BT61 9DG, UK

⁴⁰ Mullard Space Science Laboratory, Department of Space and Climate Physics, University College London, Holmbury St. Mary, Dorking, Surrey RH5 6NT, UK

⁴¹ Gruppo Astrofili Montelupo, Via San Vito 60, I-50056 Montelupo Fiorentino (FI), Italy

⁴² Public Observatory Buchloe, Alois-Reiner-Str. 15b, D-86807 Buchloe, Germany

⁴³ Department of Medical Physics and Acoustics, University of Oldenburg, D-26111 Oldenburg, Germany

⁴⁴ Astronomical Research Institute, 7168 NCR 2750E, Ashmore, IL 61912, USA

⁴⁵ H.O.B. Astronomical Observatory, Via Buca dei Tassi 13, I-50050 Capraia Fiorentina (FI), Italy

⁴⁶ Southern Observatory for Near Earth Asteroids Research, Oliveira, Brazil

⁴⁷ Shanghai Astronomical Observatory, Chinese Academy of Science, Shanghai 200030, People's Republic of China

⁴⁸ Tartu Observatory, University of Tartu, Observatooriumi 1, Tõravere, 61602, Estonia

⁴⁹ Korea Astronomy and Space Science Institute, 776, Daedeokdae-ro, Yuseong-gu, Daejeon 34055, Republic of Korea

⁵⁰ Golden Ears Observatory, 22938 Vista Ridge Dr., Maple Ridge, BC V4R 2X3, Canada

- ⁵¹ Purple Mountain Observatory, Chinese Academy of Sciences, Nanjing, 210023, People's Republic of China
⁵² University of Science and Technology of China, Hefei, 230026, People's Republic of China
⁵³ Bernezzo Observatory, Via Maggiori 28, I-12010 Bernezzo (CN), Italy
⁵⁴ Farm Cove Observatory, 2/24 Rapallo Place, Farm Cove, Auckland 2010, New Zealand
⁵⁵ Killer Rocks Observatory, HC 65 Box 2, Pie Town, NM 87827, USA
⁵⁶ GAL Hassin—Centro Internazionale per le Scienze Astronomiche, Via della Fontana Mitri, I-90010 Isnello (PA), Italy
⁵⁷ Wickede Observatory, Stemmering 5, D-44319 Dortmund, Germany
⁵⁸ Petrozavodsk State University, Lenin St., 33, 185910, Petrozavodsk, Republic of Karelia, Russia
⁵⁹ Landeher Observatory (Z43), 14 allée des Ajoncs d'Or F-22400 LANDEHEN, France
⁶⁰ Amateur astronomer, Russia
⁶¹ Remote observer of the Liverpool Telescope, La Palma, Spain
⁶² iTelescope.Net observatories: New Mexico Skies, Mayhill, NM, USA
⁶³ Siding Spring Observatory, Australia
⁶⁴ Osservatorio Astronomico Nastro Verde, Via Nastro Verde, I-80067 Sorrento (NA), Italy
⁶⁵ Instituto de Física Aplicada a las Ciencias y las Tecnologías, Universidad de Alicante, San Vicente del Raspeig, E-03080, Alicante, Spain
⁶⁶ Institut de Ciències del Cosmos (ICCUB), Universitat de Barcelona (IEEC-UB), Carrer de Martí i Franquès, 1, E-08028 Barcelona, Spain
⁶⁷ Toni Scarmato's Observatory, Via U. Foscolo 3, I-89817 San Costantino di Briatico (VV), Italy
⁶⁸ Arkansas Sky Observatories, ASO Scientific Studies Inc., 73 Tanyard Springs Rd., Petit Jean Mountain, AR 72110, USA
⁶⁹ NOAK Observatory, Delfon 2 Stavraki, Ioannina, 45500, Greece
⁷⁰ Dipartimento di Fisica e Astronomia, Università di Bologna, Via Zamboni 33, I-40126 Bologna, Italia
⁷¹ Physics and Astronomy, The University of Western Ontario, 1151 Richmond St., London, ON N6A 3K7, Canada
 Received 2023 June 29; revised 2023 August 24; accepted 2023 September 18; published 2023 November 2

Abstract

The Earth close approach of near-Earth asteroid 2005 LW3 on 2022 November 23 represented a good opportunity for a second observing campaign to test the timing accuracy of astrometric observation. With 82 participating stations, the International Asteroid Warning Network collected 1046 observations of 2005 LW3 around the time of the close approach. Compared to the previous timing campaign targeting 2019 XS, some individual observers were able to significantly improve the accuracy of their reported observation times. In particular, U.S. surveys achieved good timing performance. However, no broad, systematic improvement was achieved compared to the previous campaign, with an overall negative bias persisting among the different observers. The calibration of observing times and the mitigation of timing errors should be important future considerations for observers and orbit computers, respectively.

Unified Astronomy Thesaurus concepts: Asteroids (72); Near-Earth objects (1092); Optical telescopes (1174); Astrometry (80)

1. Introduction

The International Asteroid Warning Network (IAWN)⁷² was established to create an international group of organizations involved in detecting, tracking, and characterizing near-Earth objects. The IAWN has conducted multiple observational campaigns to exercise the preparedness of the international community for the different components of the mitigation response of a potential impact hazard: discovery, recovery and tracking, physical characterization, and risk assessment (Reddy et al. 2019, 2022a, 2022b).

In order to assess the quality of the observational data used in the orbit determination process, the 2021 campaign targeted asteroid 2019 XS during its close approach to Earth (Farnocchia et al. 2022). Because of the asteroid's high rate of motion in the sky, timing errors significantly contributed to the astrometric positional errors in the plane of sky. Timing errors can be due to several reasons, such as infrequent or unsuccessful synchronization, a delay between the command to open the shutter and the actual motion of the device, a finite travel time of the shutter over the focal plane, numerical rounding, or confusion between the exposure start time and


mid-time. By breaking down the plane-of-sky positional errors in the along-track (i.e., aligned with the plane-of-sky motion) and cross-track (i.e., perpendicular to the plane-of-sky motion) directions, Farnocchia et al. (2022) assessed the accuracy of the time of the observations reported to the Minor Planet Center (MPC). The timing errors were typically smaller than 1 s. However, there was an overall negative bias; i.e., the reported observation times were earlier than they should have been, on average.

Thanks to the possibility of reporting astrometric uncertainties using the ADES format (Chesley et al. 2017),⁷³ a second outcome of the 2019 XS campaign was that of validating the reliability of the reported uncertainties by comparing them to the cross-track errors, which are not affected by timing or trailing and therefore reflect purely positional errors. A fraction of the reported uncertainties appeared to be optimistic, especially when smaller than 0".2, thus suggesting that some sources of error are not fully captured in the uncertainty estimation process.

To address both timing accuracy and uncertainty quantification issues, Farnocchia et al. (2022) recommended calibrating observation times against GNSS satellites⁷⁴ and presented a recipe to derive realistic, conservative uncertainties.

Near-Earth asteroid 2005 LW3 was discovered in 2005 June by the Siding Spring Survey (MPEC 2005-L19).⁷⁵ The

⁷² <https://iawn.net>

 Original content from this work may be used under the terms of the [Creative Commons Attribution 4.0 licence](https://creativecommons.org/licenses/by/4.0/). Any further distribution of this work must maintain attribution to the author(s) and the title of the work, journal citation and DOI.

⁷³ <https://github.com/IAU-ADES/ADES-Master>

⁷⁴ https://www.projectpluto.com/gps_find.htm

⁷⁵ <https://www.minorplanetcenter.net/mpec/K05/K05L19.html>

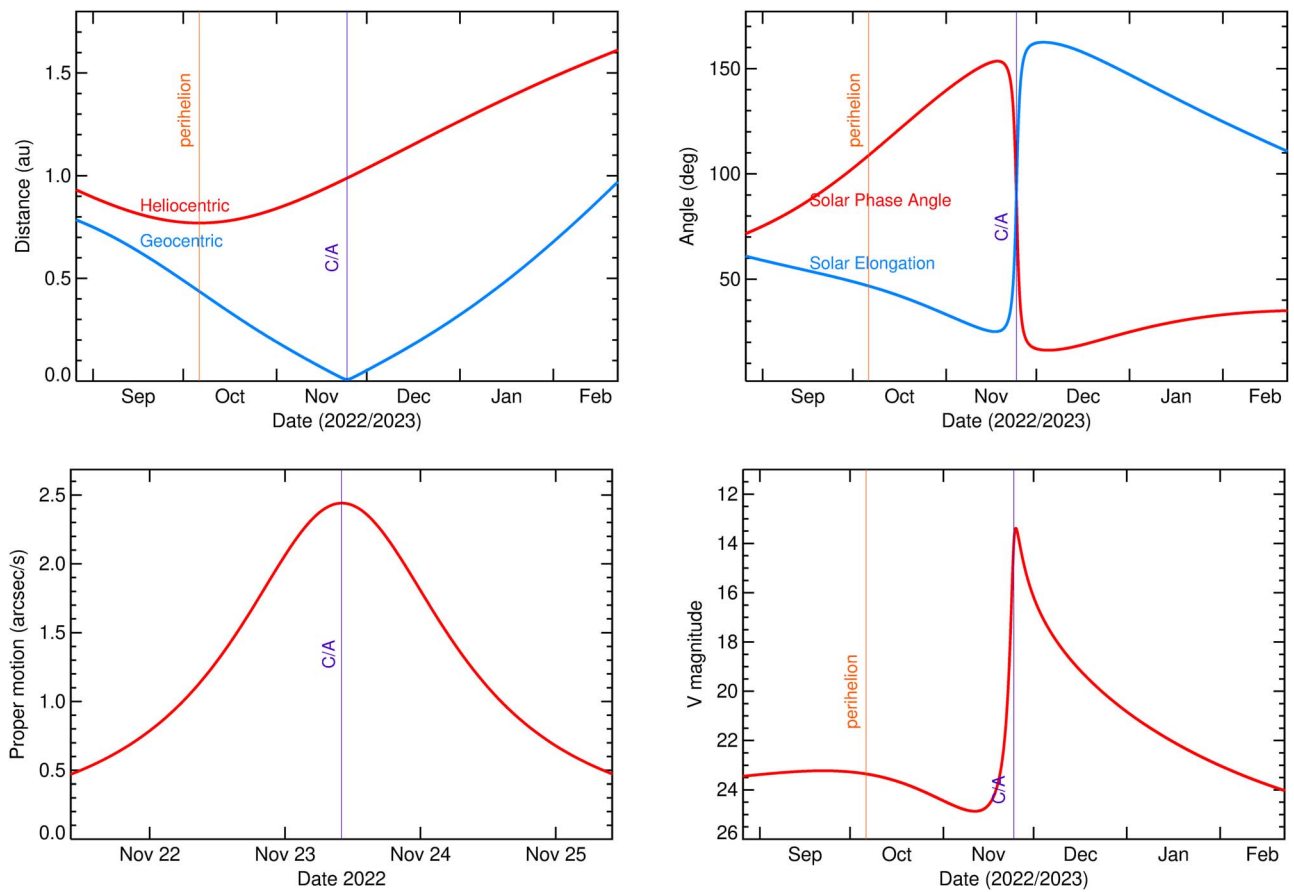


Figure 1. Geocentric and heliocentric distance (top left), solar elongation and phase angle (top right), plane-of-sky rate of motion (bottom left), and V-band magnitude (bottom right) of 2005 LW3 as a function of time. The vertical lines correspond to the times of perihelion and closest approach to Earth.

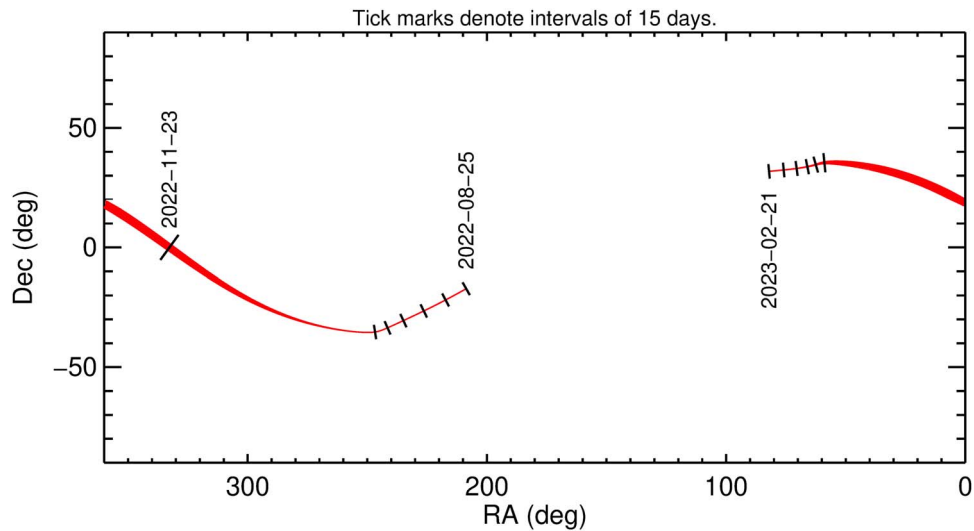


Figure 2. R.A. and decl. of 2005 LW3 as a function of time. The thickness of the line is related to the brightness of the object.

asteroid, with an inferred diameter between 100 and 300 m based on its absolute magnitude $H = 21.7$, made a close approach to Earth on 2022 November 23 at a distance of 1.1 million km (about 3 lunar distances; see top left panel of Figure 1) from the geocenter. Figures 1 and 2 show the observing conditions for 2005 LW3 around the close approach.

The asteroid was bright enough (bottom right panel of Figure 1) to be easily observable, moving rapidly in the sky (albeit not quite as fast as 2019 XS), and more accessible from the Northern Hemisphere (Figure 2). We aimed to conduct a timing campaign in the second half of 2022, and 2005 LW3 was the only candidate with a plane-of-sky rate of motion greater than

Table 1
List of Participating Observatories and Number of Observations Collected as Part of the Campaign between 2022-11-21.0 UTC and 2022-11-25.0 UTC

Code	Name	No. of Obs.	Code	Name	No. of Obs.
104	San Marcello Pistoiese	19	L28	ISON-Castelgrande Observatory	16
130	Lumezzane	25	L34*	Galhassin Robotic Telescope, Isnello	9
186*	Kitab	13	L63	HOB Observatory, Capraia Fiorentina	6
203*	GiaGa Observatory	18	L73*	Beato Ermanno Observatory, Impruneta	6
204	Schiaparelli Observatory	10	L80*	SpringBok Observatory, Tivoli	5
215*	Buchloe	11	L92	San Costantino	33
511	Haute Provence	7	M22†	ATLAS South Africa, Sutherland	5
654*	Table Mountain Observatory, Wrightwood-PHMC	3	M33*	OWL-Net, Mitzpe Ramon	22
675	Palomar Mountain	4	N50*	Himalayan Chandra Telescope, IAO, Hanle	10
703*†	Catalina Sky Survey	18	N82*	Multa Observatory	18
807	Cerro Tololo Observatory, La Serena	11	O68	LW-2, NAOC-Zhongwei	10
954	Teide Observatory	5	O72	OWL-Net, Songino	4
A29	Santa Maria a Monte	21	O85	LiShan Observatory, Lintong	7
B66	Osservatorio di Casasco	5	P65	OWL-Net, Daedeok	33
C40*	Kuban State University Astrophysical Observatory	3	P72	OWL-Net, Mt. Bohyun	32
C65*	Osservatori Astronomico del Montsec	8	Q62	iTelescope Observatory, Siding Spring	10
C77	Bernezzo Observatory	8	T05*†	ATLAS-HKO, Haleakala	5
C82	Osservatorio Astronomico Nastro Verde, Sorrento	9	T08*†	ATLAS-MLO, Mauna Loa	14
D03	Rantiga Osservatorio, Tincana	12	T12*	University of Hawaii 88-inch telescope, Maunakea	12
D29*†	Purple Mountain Observatory, XuYi Station	30	U55	Golden Ears Observatory, Maple Ridge	6
E10	Siding Spring-Faulkes Telescope South	12	U74	JPL SynTrack Robotic Telescope 2, Auberry	5
E85*	Farm Cove	46	V00	Kitt Peak-Bok	16
F52*†	Pan-STARRS 2, Haleakala	2	V06*	Catalina Sky Survey-Kuiper	14
G01	Universitaetssternwarte Oldenburg	16	V15*	OWL-Net, Mt. Lemmon	27
G17	BAS Observatory, Scandicci	4	V17*	Leo Observatory, Tucson	18
G33*	Wickede	33	V20*	Killer Rocks Observatory, Pie Town	53
G34*	Oberfrauendorf	32	V28	Deep Sky West Observatory, Rowe	5
G96*†	Mt. Lemmon Survey	10	V37*	McDonald Observatory-LCO ELP	2
H06	iTelescope Observatory, Mayhill	8	V39*	McDonald Observatory-LCO ELP B	6
H21	Astronomical Research Observatory, Westfield	8	W34*	Squirrel Valley Observatory, Columbus	6
H45	Arkansas Sky Obs., Petit Jean Mountain South	18	W68†	ATLAS Chile, Rio Hurtado	5
I52*	Steward Observatory, Mt. Lemmon Station	16	W87	Cerro Tololo-LCO C	3
J04	ESA Optical Ground Station, Tenerife	6	W98*	Polonia Observatory, San Pedro de Atacama	7
J13	La Palma-Liverpool Telescope	6	Y00*	SONEAR Observatory, Oliveira	21
J69	North Observatory, Clanfield	13	Z01	OWL-Net, Oukaimeden	15
K19	PASTIS Observatory, Banon	12	Z21	Tenerife-LCO Aqawan A #1	1
K38	M57 Observatory, Saltrio	3	Z23*	Nordic Optical Telescope, La Palma	25
K40	Altdorf	4	Z31*	Tenerife Observatory-LCO A, Tenerife	6
K47	BSCR Observatory, Santa Maria a Monte	8	Z43*	Landehen	10
K63	G. Pascoli Observatory, Castelvechio Pascoli	16	Z80*	Northolt Branch Observatory	9
L02*	NOAK Observatory, Stavradi	6	Z84*	Calar Alto-Schmidt	10

Note. A † indicates surveys, while an asterisk indicates stations that also participated in the 2019 XS campaign (Farnocchia et al. 2022).

$2'' \text{ s}^{-1}$ (bottom left panel of Figure 1) that could be observed after the encounter (high elongation and bright, as shown by the top right and bottom left panels of Figure 1, respectively), thus constraining the orbit enough to reliably analyze the timing errors. We therefore selected 2005 LW3 as a target for a second IAWN timing campaign.⁷⁶

2. Observations

Table 1 lists the 82 stations that participated in the campaign, and Figure 3 shows their geographical location. The broad geographical coverage is encouraging in terms of ensuring that observers are available in case of short observing windows that limit favorable observing conditions to only specific locations. Thirty-eight stations participated in both the 2019 XS campaign and the 2005 LW3 one, while 33 stations only participated in

the 2019 XS campaign, and 44 stations only participated in the 2005 LW3 campaign.

We observed 2005 LW3 from 2022 November 21.9 UTC to 25.0 UTC, i.e., the days around the closest approach, when the object was moving faster in the sky. The earliest campaign observations were collected by SONEAR Observatory in Brazil, and a total of 1046 astrometric observations of the plane-of-sky position of 2005 LW3 were reported by campaign participants to the MPC. The observations can be found in the MPC's Daily Orbit Update Minor Planet Electronic Circulars (MPECs) 2022-W151,⁷⁷ 2022-W161,⁷⁸ 2022-W171,⁷⁹ 2022-W190,⁸⁰ 2022-W220,⁸¹

⁷⁶ <https://iawn.net/obscomp/2005LW3>

⁷⁷ <https://www.minorplanetcenter.net/mpec/K22/K22WF1.html>

⁷⁸ <https://www.minorplanetcenter.net/mpec/K22/K22WG1.html>

⁷⁹ <https://www.minorplanetcenter.net/mpec/K22/K22WH1.html>

⁸⁰ <https://www.minorplanetcenter.net/mpec/K22/K22WJ0.html>

⁸¹ <https://www.minorplanetcenter.net/mpec/K22/K22WM0.html>

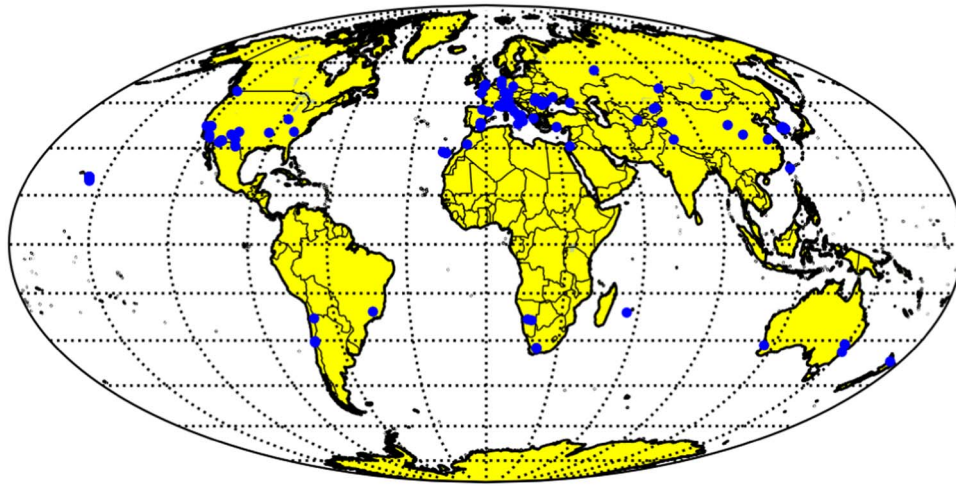


Figure 3. Locations of the 82 ground-based observation sites that participated in the campaign.

Table 2
Number of Campaign Observations for Each Star Catalog

Star Catalog	Number of Observations	Fraction	References
Gaia-DR2	650	62.1%	Gaia Collaboration et al. (2018)
Gaia-EDR3	242	23.1%	Gaia Collaboration et al. (2021)
Gaia-DR3	26	2.5%	Gaia Collaboration et al. (2023)
ATLAS-2	14	1.3%	Tonry et al. (2018)
UCAC-4	87	8.3%	Zacharias et al. (2013)
UCAC-3	14	1.3%	Zacharias et al. (2010)
Tycho-2	13	1.2%	Høg et al. (2000)

2022-W235,⁸² 2022-W252,⁸³ 2022-W283,⁸⁴ 2022-X16,⁸⁵ 2022-X49,⁸⁶ and 2022-X51.⁸⁷

The majority (664, i.e., 63%) of these observations were reported using the ADES format, thus including uncertainty information. The full ADES records can be accessed using the xml version of the abovementioned MPECs.⁸⁸

Table 2 shows the star catalogs used to reduce the astrometric observations from this campaign. Of the observations, 89% were reduced using one of the Gaia star catalogs or ATLAS-2, which uses Gaia sources, thus removing any concern for star catalog biases (e.g., Eggl et al. 2020) affecting the accuracy of the measured astrometric positions. Older, less accurate catalogs should be deprecated for the purpose of astrometric reduction.

3. Analysis of the Residuals

We analyzed the astrometry collected as part of the campaign against JPL solution 27 (Table 3). This orbital solution for 2005 LW3 is based on the optical data reported to the MPC through 2023 January 8.⁸⁹ To keep timing errors from biasing the orbital solution, around the November 22 close approach, we only selected single detections from J04, T12,

⁸² <https://www.minorplanetcenter.net/mpec/K22/K22WN5.html>

⁸³ <https://www.minorplanetcenter.net/mpec/K22/K22WP2.html>

⁸⁴ <https://www.minorplanetcenter.net/mpec/K22/K22WS3.html>

⁸⁵ <https://www.minorplanetcenter.net/mpec/K22/K22X16.html>

⁸⁶ <https://www.minorplanetcenter.net/mpec/K22/K22X49.html>

⁸⁷ <https://www.minorplanetcenter.net/mpec/K22/K22X51.html>

⁸⁸ e.g., <https://www.minorplanetcenter.net/mpec/K22/K22WF1.xml>.

⁸⁹ https://minorplanetcenter.net/db_search/show_object?utf8=%E2%9C%93&object_id=2005+LW3

Table 3
JPL Orbit Solution 27

Parameter	Value
Eccentricity	$0.4621568200 \pm 1.78 \times 10^{-8}$
Perihelion distance	$0.7696897321 \pm 2.36 \times 10^{-8}$ au
Time of perihelion	2022-10-05.289035444 TDB $\pm 8.46 \times 10^{-7}$ days
Longitude of node	$59.60615392 \pm 2.32 \times 10^{-6}$ deg
Argument of perihelion	$288.23870605 \pm 2.89 \times 10^{-6}$ deg
Inclination	$6.04822261 \pm 4.74 \times 10^{-6}$ deg
Yarkovsky parameter A_2	$-6.24 \times 10^{-14} \pm 1.45 \times 10^{-14}$ au day ⁻²

Note. The osculating epoch is 2022 July 19 TDB, and the orbital elements refer to the IAU76 ecliptic frame (Seidelmann 1977). Error bars correspond to formal 1σ uncertainties. The solution is based on 123 optical observations from 2005 June 5 to 2023 January 8 and four radar delay and three radar Doppler observations.

D03, and V28. These four stations calibrated their timing to better than 0.1 s by observing GNSS satellites⁹⁰ prior to observing 2005 LW3. Finally, we included radar observations collected between 2022 November 22 and 27.⁹¹

We projected the astrometric residuals in the along- and cross-track directions, i.e., in the directions parallel and perpendicular to the motion of 2005 LW3 in the sky. The exact procedure is presented in detail in Farnocchia et al. (2022) and is therefore not repeated here. The cross-track direction is not affected by timing errors and so is informative about the purely astrometric positional errors. For each tracklet,

⁹⁰ https://www.projectpluto.com/gps_find.htm

⁹¹ <https://ssd.jpl.nasa.gov/sb/radar.html>

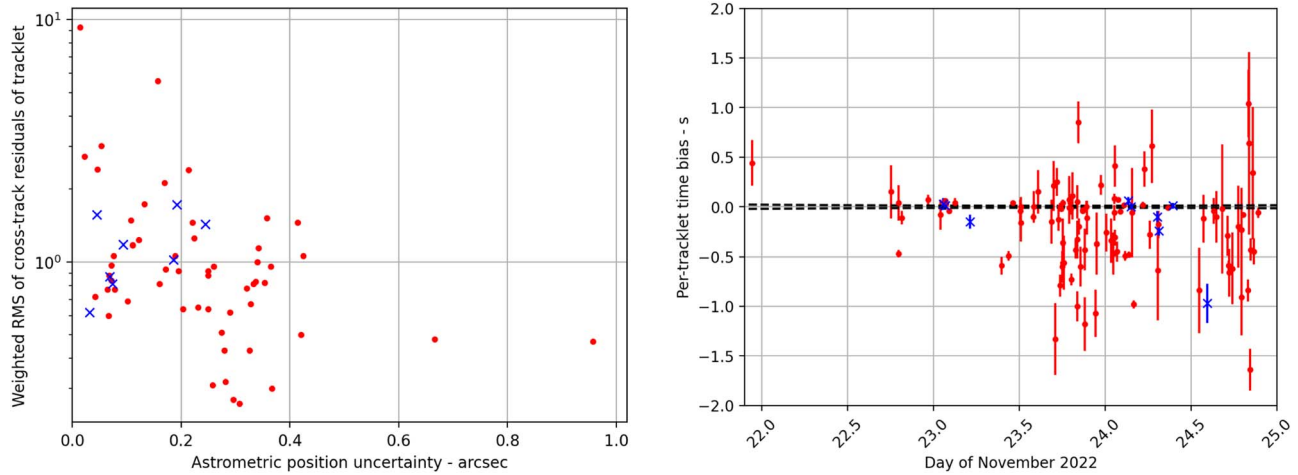


Figure 4. Left: weighted rms of the cross-track residuals of each tracklet as a function of the astrometric position uncertainties. Right: estimated mean timing error for each tracklet of observations considered in our analysis. Crosses correspond to survey data, and dots correspond to follow-up data. Three outliers with timing errors between 2 and 4 s fall outside the plot. The two dashed lines correspond to the orbital uncertainty mapped into the along-track direction in the plane of sky and converted to time using the rate of motion.

i.e., an arc of consecutive observations of the same target from the same station closely spaced in time, typically within an hour, with uncertainties reported in ADES, the left panel of Figure 4 shows the weighted rms, which is the rms of the residuals normalized by the observer-provided uncertainty. A weighted rms of 1 means that the claimed uncertainty exactly matches the noise in the data, a weighted rms < 1 means that the reported uncertainties are overestimated, while a weighted rms > 1 means that the noise in the data is not captured by the reported uncertainties. As already found for 2019 XS (Farnocchia et al. 2022), the reported uncertainties tend to become more and more optimistic (up to a factor of 10) as they become smaller, especially when $< 0''.2$. The implication is that some error sources may not be fully captured in the uncertainty quantification.

The timing error is the along-track residual divided by the rate of motion. The right panel of Figure 4 shows the timing error of each tracklet of observations collected as part of the campaign. As already noticed for the 2019 XS campaign (Farnocchia et al. 2022), most tracklets have timing errors within 1 s. For 28 stations, there is no measurable time bias, while 26 stations have biases within 0.5 s. Seven participating stations have timing errors exceeding 1 s, though one of them has large and biased cross-track errors, so positional errors could fully explain its along-track errors without invoking timing errors. Overall, there is still a negative time bias of around -0.2 s, which means that, on average, the reported times are 0.2 s earlier than they should be.

Despite the persistence of an overall time bias, it is worth noting that 14 stations managed to significantly improve compared to the 2019 XS campaign, while a couple stations performed worse than in the previous campaign. As an example, Leo Observatory (station code V17) did not report uncertainties and had a -0.6 s timing bias for the observations of 2019 XS during the 2021 close approach. For this campaign, V17 adopted the recommendations by Farnocchia et al. (2022) to quantify the uncertainties and calibrate the timing using GNSS satellites, which helped improve the observation accuracy. The V17 results can be seen in Figure 5. The right panel shows the cross-track residuals of V17, which are small and consistent with the uncertainties as reported by the

observer using the ADES format. The right panel shows the timing errors, which are statistically consistent with zero. The first five astrometric positions were derived by stacking multiple images, while the last five were derived from single images. Due to the brightness of 2005 LW3, stacking was not necessary, but measuring positions using both approaches shows that no timing error is being introduced by the stacking procedure. When stacking, it is important to keep in mind that separate sets of exposures should be used for different stacks.

Surveys in the United States generally achieved good timing performance (see Figure 4). The Catalina Sky Survey (Christensen et al. 2018; station codes 703 and G96) has errors of the order of a few hundredths of a second, statistically consistent with zero. The same is true for Pan-STARRS (Wainscoat et al. 2022; station code F52), which represents a significant improvement over the -0.5 s bias observed during the 2019 XS campaign. The ATLAS survey (Tonry et al. 2018) has errors between -0.1 and -0.2 s for the stations in Hawaii (codes T05 and T08) and essentially no bias for the two more recent stations in South Africa (code M22) and Chile (code W68).

4. Discussion

Timing errors become a key consideration when observing objects close to Earth that move rapidly in the sky. The faster the object, the larger the astrometric position displacement induced by a timing error. If not mitigated, timing errors affect the accuracy of orbits determined by fitting these observations. The effect becomes even more severe if the timing errors are systematic, not only for individual tracklets but even across different stations and nights.

Measures can be taken as part of the orbit determination process to mitigate timing errors. For example, Farnocchia et al. (2022) described how to augment an observation's covariance matrix to account for a time uncertainty. For this very reason, the ADES format includes fields that observers can use to communicate estimated random and systematic errors in time and other fields to be used by orbit computers to set time biases and weights. Therefore, debiasing and weighting schemes can be developed based on statistical analysis of the residuals analogous to the statistical schemes

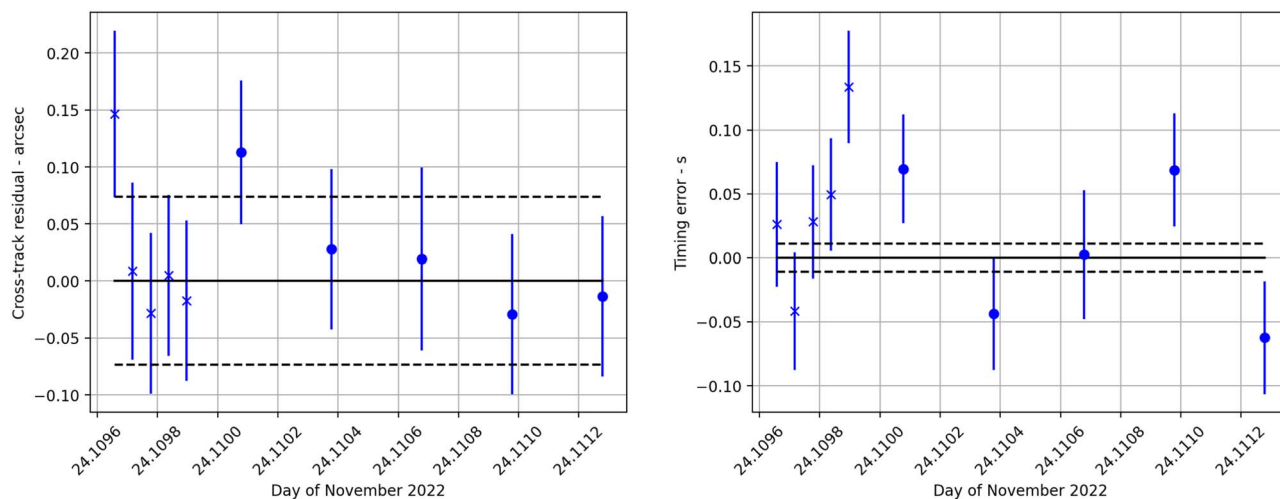


Figure 5. Cross-track (left panel) and timing (right panel) errors (crosses and dots) and 1σ error bars for a tracklet of observations collected by V17 during the campaign. The two dashed lines correspond to the orbit solution uncertainty in the along-track direction scaled by the rate of motion. Crosses correspond to positions obtained by stacking images, while dots are for positions measured from single images.

devised for the purely positional terms of the astrometric errors (Vereš et al. 2017; Ettl et al. 2020). However, it remains preferable for timing problems to be addressed at the source, with observers correcting for time biases directly, so that the information from astrometric observations can be fully leveraged. To support the quantification and resolution of these biases, we provided each participating observer with a detailed report of the results from this campaign.

Compared to the first timing campaign targeting 2019 XS (Farnocchia et al. 2022), some observers were able to report more accurate observation times. However, there was no clear, systematic improvement, and an overall negative time bias persists. This is especially true for follow-up observers. Thus, more work is needed to improve timing accuracy, e.g., by ensuring that observers take full advantage of tools like Project Pluto’s GNSS page⁹² to properly and regularly calibrate their timing.

A similar conclusion holds about the reliability of astrometric uncertainties. It is encouraging to see a larger fraction of the observing community adopting the ADES format and reporting their uncertainty estimates, which provide key information for orbit computers to properly weight the data. However, such uncertainties can prove optimistic, especially when $<0''.2$. Astrometric weighting schemes will need to account for this issue, e.g., by incorporating some (possibly station-specific) minimum credible error.

Future campaigns will be announced on the IAWN website⁹³ and possibly with an editorial notice by the MPC.

Acknowledgments

Part of this research was conducted at the Jet Propulsion Laboratory, California Institute of Technology, under a contract with the National Aeronautics and Space Administration (80NM0018D0004). This research has made use of data and services provided by the International Astronomical Union’s Minor Planet Center at the Smithsonian Astrophysical Observatory and the Small Bodies Node of the NASA Planetary Data System (PDS), managed at the University of

Maryland and funded by NASA’s Planetary Defense Coordination Office through PDS cooperative agreement 80NSSC22M0024 and UMD-SAO subaward 106075-Z6415201. B.T.B. is supported by an appointment to the NASA Postdoctoral Program at the NASA Goddard Space Flight Center, administered by Oak Ridge Associated Universities under contract with NASA. SED Machine is based upon work supported by the National Science Foundation under grant No. 1106171. T.S.R. acknowledges funding from the NEO-MAPP project (H2020-EU-2-1-6/870377). This work was (partially) supported by the Spanish MICIN/AEI/10.13039/501100011033 and “ERDF A way of making Europe” by the European Union through grant PID2021-122842OB-C21 and the Institute of Cosmos Sciences University of Barcelona (ICCUB, Unidad de Excelencia “María de Maeztu”) through grant CEX2019-000918-M. The Joan Oró Telescope (TJO) of the Montsec Observatory (OdM) is owned by the Catalan Government and operated by the Institute for Space Studies of Catalonia (IEEC). The Liverpool Telescope is operated on the island of La Palma by Liverpool John Moores University in the Spanish Observatorio del Roque de los Muchachos of the Instituto de Astrofísica de Canarias with financial support from the UK Science and Technology Facilities Council. This paper was partially based on observations obtained at the Optical Wide-field patrol Network (OWL-Net), which is operated by the Korea Astronomy and Space Science Institute (KASI).

Copyright 2023. California Institute of Technology.

ORCID iDs

Davide Farnocchia <https://orcid.org/0000-0003-0774-884X>
 Vishnu Reddy <https://orcid.org/0000-0001-5133-6303>
 James M. Bauer <https://orcid.org/0000-0001-9542-0953>
 Elizabeth M. Warner <https://orcid.org/0000-0003-1147-4474>
 Marco Micheli <https://orcid.org/0000-0001-7895-8209>
 Matthew J. Payne <https://orcid.org/0000-0001-5133-6303>
 Tony Farnham <https://orcid.org/0000-0002-4767-9861>
 Miguel R. Alarcon <https://orcid.org/0000-0002-8134-2592>
 Paolo Bacci <https://orcid.org/0000-0002-3105-7072>
 Roberto Bacci <https://orcid.org/0000-0002-3918-9475>

⁹² https://www.projectpluto.com/gps_find.htm

⁹³ <https://iawn.net>

Kevin Baillié  <https://orcid.org/0000-0002-2120-6388>
 Daniel Bamberger  <https://orcid.org/0000-0002-9138-2942>
 Enrico Biancalani  <https://orcid.org/0000-0002-6137-0342>
 Bryce T. Bolin  <https://orcid.org/0000-0002-4950-6323>
 David Briggs  <https://orcid.org/0000-0002-7439-3463>
 Larry Denneau  <https://orcid.org/0000-0002-7034-148X>
 Josselin Desmars  <https://orcid.org/0000-0002-2193-8204>
 Anlaug A. Djupvik  <https://orcid.org/0000-0001-6316-9880>
 Leonid Elenin  <https://orcid.org/0000-0001-9336-9648>
 Randy Flynn  <https://orcid.org/0000-0002-4562-2204>
 Mikael Granvik  <https://orcid.org/0000-0002-5624-1888>
 Bill Gray  <https://orcid.org/0000-0001-7154-3342>
 Zuri Gray  <https://orcid.org/0000-0002-6610-1897>
 Tobias Hoffmann  <https://orcid.org/0000-0003-4643-3664>
 Cristóvão Jacques  <https://orcid.org/0000-0002-3100-4632>
 Anni Kasikov  <https://orcid.org/0000-0002-1823-3975>
 Myung-Jin Kim  <https://orcid.org/0000-0002-4787-6769>
 Hee-Jae Lee  <https://orcid.org/0000-0002-6839-075X>
 Bin Li  <https://orcid.org/0000-0001-9327-0920>
 Tyler Linder  <https://orcid.org/0000-0003-2534-673X>
 James D. Neill  <https://orcid.org/0000-0002-0466-1119>
 Dong-Goo Roh  <https://orcid.org/0000-0001-6104-4304>
 Filipp D. Romanov  <https://orcid.org/0000-0002-5268-7735>
 Toni Santana-Ros  <https://orcid.org/0000-0002-0143-9440>
 Toni Scarmato  <https://orcid.org/0000-0003-2463-6268>
 Sergei Schmalz  <https://orcid.org/0000-0001-5783-3888>
 Nick Sioulas  <https://orcid.org/0000-0002-2012-1227>
 David J. Tholen  <https://orcid.org/0000-0003-0773-1888>

William Thuillot  <https://orcid.org/0000-0002-5203-6932>
 Richard Wainscoat  <https://orcid.org/0000-0002-1341-0952>
 Guy Wells  <https://orcid.org/0009-0000-6288-3150>
 Robert Weryk  <https://orcid.org/0000-0002-0439-9341>
 Hong-Suh Yim  <https://orcid.org/0000-0001-5484-4741>
 Chengxing Zhai  <https://orcid.org/0000-0002-0291-4522>

References

- Chesley, S. R., Hockney, G. M., & Holman, M. J. 2017, AAS/DPS Meeting, **49**, 112.14
 Christensen, E., Africano, B., Farneth, G., et al. 2018, AAS/DPS Meeting, **50**, 310.10
 Ettl, S., Farnocchia, D., Chamberlin, A. B., & Chesley, S. R. 2020, *Icar*, **339**, 113596
 Farnocchia, D., Reddy, V., Bauer, J. M., et al. 2022, *PSJ*, **3**, 156
 Gaia Collaboration, Brown, A. G. A., Vallenari, A., et al. 2018, *A&A*, **616**, A1
 Gaia Collaboration, Brown, A. G. A., Vallenari, A., et al. 2021, *A&A*, **649**, A1
 Gaia Collaboration, Vallenari, A., Brown, A. G. A., et al. 2023, *A&A*, **674**, A1
 Høg, E., Fabricius, C., Makarov, V. V., et al. 2000, *A&A*, **355**, L27
 Reddy, V., Kelley, M. S., Dotson, J., et al. 2022a, *Icar*, **374**, 114790
 Reddy, V., Kelley, M. S., Dotson, J., et al. 2022b, *PSJ*, **3**, 123
 Reddy, V., Kelley, M. S., Farnocchia, D., et al. 2019, *Icar*, **326**, 133
 Seidelmann, P. K. 1977, *CeMec*, **16**, 165
 Tonry, J. L., Denneau, L., Flewelling, H., et al. 2018, *ApJ*, **867**, 105
 Vereš, P., Farnocchia, D., Chesley, S. R., & Chamberlin, A. B. 2017, *Icar*, **296**, 139
 Wainscoat, R., Weryk, R., Ramanjooloo, Y., et al. 2022, AAS/DPS Meeting, **54**, 504.01
 Zacharias, N., Finch, C., Girard, T., et al. 2010, *AJ*, **139**, 2184
 Zacharias, N., Finch, C. T., Girard, T. M., et al. 2013, *AJ*, **145**, 44